STEM CELLS TRANSLATIONAL MEDICINE®

PLURIPOTENT STEM CELLS

Rho Kinase Inhibition Is Essential During In Vitro Neurogenesis and Promotes Phenotypic Rescue of Human Induced Pluripotent Stem Cell-Derived Neurons With Oligophrenin-1 Loss of Function

CLAUDIA COMPAGNUCCI,[a] SABINA BARRESI,[a] STEFANIA PETRINI,[b] PIERRE BILLUART,[c] GIORGIA PICCINI,[d] PIETRO CHIURAZZI,[e] PAOLO ALFIERI,[d] ENRICO BERTINI,[a] GINEVRA ZANNI[a]

Key Words. Oligophrenin-1 • In vitro neurogenesis • Rho-kinase signaling • ROCK inhibitors (fasudil, Y-27632)

ABSTRACT

Rho-GTPases have relevant functions in various aspects of neuronal development, such as differentiation, migration, and synaptogenesis. Loss of function of the oligophrenin-1 gene (*OPHN1*) causes X-linked intellectual disability with cerebellar hypoplasia and leads to hyperactivation of the rho kinase (ROCK) pathway. ROCK mainly acts through phosphorylation of the myosin phosphatase targeting subunit 1, triggering actin-myosin contractility. We show that during in vitro neurogenesis, ROCK activity decreases from day 10 until terminal differentiation, whereas in OPHN1-deficient human induced pluripotent stem cells (h-iPSCs), the levels of ROCK are elevated throughout differentiation. ROCK inhibition favors neuronal-like appearance of h-iPSCs, in parallel with transcriptional upregulation of nuclear receptor *NR4A1*, which is known to induce neurite outgrowth. This study analyzed the morphological, biochemical, and functional features of OPHN1-deficient h-iPSCs and their rescue by treatment with the ROCK inhibitor fasudil, shedding light on the relevance of the ROCK pathway during neuronal differentiation and providing a neuronal model for human OPHN1 syndrome and its treatment. STEM CELLS TRANSLATIONAL MEDICINE *2016;5:860–869*

SIGNIFICANCE

The analysis of the levels of rho kinase (ROCK) activity at different stages of in vitro neurogenesis of human induced pluripotent stem cells reveals that ROCK activity decreases progressively in parallel with the appearance of neuronal-like morphology and upregulation of nuclear receptor *NR4A1*. These results shed light on the role of the ROCK pathway during early stages of human neurogenesis and provide a neuronal stem cell-based model for the treatment of OPHN1 syndrome and other neurological disorders due to ROCK dysfunction.

INTRODUCTION

Neurogenesis is the developmental process that determines differentiation of neural stem cells into glial and neuronal cells and orchestrates their organization into finely regulated and functionally integrated networks that require cytoskeletal reorganization and transcriptional regulation [1]. Rho-GTPase family proteins (rho, Rac, Cdc42) have relevant functions in regulating various aspects of neuronal development (i.e., differentiation, migration, and synaptogenesis). Rho-GTPase activity is modulated through positive (GTPase-activating proteins) and negative (guanine nucleotide exchange factors or guanine nucleotide dissociation inhibitors) regulators [2]. RhoA activates rho kinase (ROCK), which directly phosphorylates the myosin regulatory light chain (MLC) kinase (MLCK) and the myosin-binding subunit (MYPT1) of the MLC phosphatase, thereby inhibiting its catalytic activity and modulating actin polymerization and actin-myosin contractility [3].

Dysfunction of several proteins of the rho-GTPase signaling network has been involved in genetic disorders of cognition and the nervous system [4]. The human oligophrenin-1 gene (*OPHN1*) gene is located on chromosome Xq12, encompasses 25 exons, and is translated into a protein of 802 amino acids (corresponding to coding exons 2–24). *OPHN1* was first identified in a female patient showing mild intellectual disability and carrying a (X;12)(q11;q15) translocation, which encodes a rho-GTPase-activating protein that promotes GTP hydrolysis and is expressed

[a]Unit of Neuromuscular and Neurodegenerative Disorders, Department of Neurosciences, [b]Research Laboratories, Confocal Microscopy Core Facility, and [d]Unit of Child Neuropsychiatry, Department of Neurosciences, Bambino Gesù Children's Hospital, Istituti di Ricovero e Cura a Carattere Scientifico, Rome, Italy; [c]Department of Genetic and Development, Institut Cochin, Université Paris Descartes, Paris, France; [e]Institute of Human and Medical Genetics, Catholic University, Rome, Italy

Correspondence: Ginevra Zanni, M.D., Ph.D., Unit of Neuromuscular and Neurodegenerative Disorders, Bambino Gesù Children's Hospital, Istituti di Ricovero e Cura a Carattere Scientifico, 15 viale San Paolo, 00146 Rome, Italy. Telephone: 00390668504290; E-Mail: ginevra.zanni@opbg.net

Received October 16, 2015; accepted for publication February 23, 2016; published Online First on May 9, 2016.

1066-5099/2016/$20.00/0

http://dx.doi.org/10.5966/sctm.2015-0303

in neurons at the pre- and postsynaptic level [5]. Since then, several mutations of this gene have been reported in X-linked intellectual disability (MIM #300486) associated with cerebellar hypoplasia [6, 7]. OPHN1 downregulates the RhoA/ROCK signaling pathway, repressing its inhibitory activity on synaptic vesicle recycling and postsynaptic α-internalization of amino-3-hydroxy-5-methyl-4-isoxazolepropionic acid receptor [8, 9]. The importance of OPHN1 for brain development and function has been demonstrated in mice, in which *ophn1*-defective adult neurons show dendritic spine immaturity and alterations in synaptic plasticity; these are partly rescued by administration of the ROCK inhibitor Y-23632 [8, 10]. Ophn1 also interacts with endophilin A1, a protein implicated in membrane curvature generation in clathrin-mediated synaptic vesicle endocytosis (SVE) [11].

The development of human induced pluripotent stem cell (iPSC) technology offers the possibility of controlling neuronal differentiation in vitro and gathering relevant details on the regulation of human neurogenesis. Several studies have shown show that administration of the ROCK inhibitor Y-27632 to human pluripotent cells decreases dissociation-dependent apoptosis, and recently Y-27632 supplementation was found to promote neuronal-like differentiation of human adipose stem cells; in contrast, lysophosphatidic acid (LPA), which hyperactivates the ROCK pathway, inhibits neuronal differentiation and expansion of human embryonic stem cells (hESCs) [12–14]. To better clarify the role of ROCK signaling in cellular physiology and disease, we analyzed the levels of ROCK activity during in vitro neurogenesis of iPSCs and tested the effects of Y-27632 supplementation on fibroblast-derived human iPSCs. We generated iPSCs from fibroblast cell lines of two patients belonging to two different families with OPHN1 loss of function [15, unpublished data], as well as two control cell lines; we differentiated these into neurons to explore their biochemical, cellular, and functional phenotype before and after treatment with fasudil (HA1077), a ROCK inhibitor that has been used as an antihypertensive drug in Japan since 1995 [16].

Materials and Methods

Ethics Statement

The study was revised and approved by the local institutional review board of Bambino Gesù Children's Hospital of Rome, Italy, which regulates the use of human samples for experimental studies. Informed consent was obtained from all the patients and their parents for the use of biological samples for research purposes.

Derivation of *OPHN1*-Mutated iPSCs

Human fibroblasts obtained from skin biopsy samples of two patients with OPHN1 syndrome and loss-of-function mutations in the *OPHN1* gene (IVS4+1G > C and IVS7+2,3 del TA, respectively) were used to generate *OPHN1*-mutated iPSCs. These iPSC lines were named P1 and P2. The control iPSC line was derived from fibroblasts from the father of the patient from whom P1 was derived (C1). C2 was used to indicate control iPSCs that were purchased from System Biosciences (Palo Alto, CA, https://www.systembio.com/) and derived from a healthy male individual. The *OPHN1*-mutated and control iPSCs were derived from human fibroblasts and reprogrammed by using the nonintegrating episomal technology (minicircle DNA and mc-iPS cells, catalog no. SC301A-1; EuroClone, Pero, Italy, http://www.euroclonegroup.it/). The episomal reprogramming method was performed, following manufacturer's instructions, through nucleoporation (followed by transfection) of human fibroblasts with the circular nonviral DNA elements encoding for NANOG, SOX2, OCT4, and Lin28. The characterization and the pluripotency assay of these iPSC lines were performed by System Biosciences (supplemental online Figs. 1 and 2, respectively).

Maintenance and Differentiation of iPSCs

After thawing, iPSCs were grown on mouse embryonic fibroblasts (Thermo Fisher Scientific Life Sciences, Waltham, MA, http://www.thermofisher.com) for two passages and then in feeder-free condition using Matrigel (BD Biosciences, San Jose, CA, http://www.bdbiosciences.com) in mTeSR1 (StemCell Technologies, Vancouver, BC, Canada, http://www.stemcell.com/). When the iPSCs are 70%–80% confluent, they are passaged 1:4 and transferred to new wells in feeder-free condition and incubated at 37°C, 5% CO_2; the medium is changed every day, and the cells split every 3 days. For the differentiation assays, iPSC colonies are dissociated and the cells are then plated at a density of 1,000 cells per cm^2 into a chemically defined medium [17].

Differentiation of iPSCs Into Cortical Neurons

The protocol for cortical neuron differentiation has been adapted from the method of Zeng et al. [18]. Cells are kept in a medium containing DMEM/F12, N2 supplement, and 2 μg/ml heparin for 16 days. On the 17th day, the medium is be replaced with neural basal medium supplemented with N2, B27, brain-derived neurotrophic factor (BDNF) (10 ng/ml), glial cell-derived neurotrophic factor (10 ng/ml), and insulin-like growth factor-1 (10 ng/ml) until day 24.

Differentiation of iPSCs Into Cerebellar Neurons

The procedure for cerebellar neuron differentiation has been adapted from the method of Erceg et al. [19]. When cells are 60% confluent, the proliferating medium is replaced with DMEM/F12, N2 supplement, 1 mg/ml heparin, fibroblast growth factor (FGF)-8 (100 ng/ml), and retinoic acid (0.1 μM); this medium was changed every day for 7 days. On the eighth day, the culture medium was replaced with basal medium Eagle (BME); insulin, transferrin, selenium; FGF-8 (10 ng/ml); FGF-4 (100 ng/ml); and FGF-2 (20 ng/ml) and left for 2 days. On day 10, the old medium was replaced with BME, FGF-8 (100 ng/ml), WNT1 (50 ng/ml), and WNT3A (50 ng/ml) and left for 6 days, with changes every other day. On day 16, the medium was replaced with BME, N2, B27, bone morphogenetic protein (BMP)-7 (100 ng/ml), BMP-6 (20 ng/ml), and growth differentiation factor (GDF)-7 (100 ng/ml); it was changed every other day for 7 days. On day 24, the medium was replaced with BME, N2, B27, BMP-7 (100 ng/ml), BMP-6 (20 ng/ml), GDF-7 (100 ng/ml), sonic hedgehog (100 ng/ml), neurotrophin-3 (100 ng/ml), BDNF (100 ng/ml), and Jagged-1 (20 ng/ml). This medium was changed every other day for 7–8 days.

Differentiation of iPSCs Into Motor Neurons

Motor neuron differentiation has been adapted from the method of Corti et al. [20]. Cells were plated at a density of 4.2–5.3 $\times$ 10^4 cells per cm^2 in NeuroCult (StemCell Technologies) for 10 days; then 0.1 μM retinoic acid was added to the cell medium, and the medium was changed every other day until day 17, when NeuroCult was supplemented not only with retinoic acid but also with 2 μM

dorsomorphin and 3 ng/ml activin A. On the 24th day, the cell medium was replaced with NeuroCult supplemented with BDNF (10 ng/ml), GNDF (2 ng/ml), dibutyryl-cAMP (400 μM), and ascorbic acid (200 μM).

Preparation of cell extracts and Western blot analyses were performed by following standard protocols. The following primary antibodies (1:1,000 dilution) were used (overnight at 4°C): rabbit OPHN1 antibody (Sigma-Aldrich, St. Louis, MO, http://www.sigmaaldrich.com), rabbit P-MYPT1 antibody (Thr 853) (Santa Cruz Biotechnology, Santa Cruz, CA, http://www.scbt.com/), rabbit MYPT1 antibody (Santa Cruz Biotechnology), anti-rabbit porin antibody (Abcam, Cambridge, U.K., http://www.abcam.com/). The density of phospho-MYPT1 against porin has been calculated after quantification by using densitometric analysis with ImageJ software (National Institutes of Health, Bethesda, MD, https://imagej.nih.gov/ij).

Immunofluorescence Analyses

For immunocytochemistry, cells were fixed with 4% paraformaldehyde for 20 minutes at room temperature, washed with PBS, and blocked with 10% bovine serum (Vector Laboratories, Burlingame, CA, http://vectorlabs.com/) and 0.1% Triton X-100 (Sigma-Aldrich). Primary antibodies included OPHN1 (1:100; made available by Pierre Billuart), β-III-TUBULIN (Cod. T2200, 1:500; Sigma-Aldrich), MATH1 (Cod. PA5-12260, 1:500; Thermo Fisher Scientific Life Sciences), SMI32 (Cod. SMI-32R, 1:200; Covance, Princeton, NJ, http://www.covance.com/), P(Thr853)-MYPT1 (Cod. 4563, 1:200; Cell Signaling Technology, Danvers, MA, http://www.cellsignal.com/), MYPT1 (Cod. 2634, 1:200; Cell Signaling Technology), P(S318)-histone deacetylase 7 (HDAC7) (Cod. ab72172, 1:100; Abcam), and VGlut (Cod. AB104898, 1:100; Abcam). Secondary antibodies were conjugated with Alexa 488, Alexa 555, or AlexaCy5 (Thermo Fisher Scientific Life Sciences). Coverslips were mounted using PBS/glycerol (1:1), visualized using a confocal microscope (FluoView FV1000; Olympus, Tokyo, Japan, http://www.olympus-global.com) and acquired with FV10-ASW software, version 2.0 (Olympus). The quantitative analysis on P-MYPT1 fluorescent intensity was performed by using ImageJ software.

RNA Isolation and Reverse Transcriptase-Polymerase Chain Reaction Analysis

Total RNA was extracted from iPSCs with the single-step acid phenol method using TRIzol (pn: 15596018; Invitrogen) according to the manufacturer's instructions. Each RNA sample was treated with recombinant DNase I (AM2235, Ambion; Thermo Fisher Scientific Life Sciences) and quantified by NanoDrop 2000 (Thermo Fisher Scientific Life Sciences). The reverse transcription reaction was performed in 20 μl starting from 1 μg of total RNA, and cDNA was generated by using the ImProm-II Reverse Transcription System (A3800; Promega, Madison, WI, https://www.promega.com/) or Superscript II reverse transcriptase (18064; Thermo Fisher Scientific Life Sciences) using random hexamers. Three independent reverse transcriptase-polymerase chain reactions (RT-PCRs) were performed for each sample.

Quantitative Real-Time PCR

Gene-specific exon-exon boundary PCR products (TaqMan gene expression assays; Thermo Fisher Scientific Life Sciences) were measured by means of a PE PRISM 7700 sequence detection system during 40 cycles (Thermo Fisher Scientific Life Sciences). Glyceraldehyde 3-phosphate dehydrogenase (GAPDH) mRNA was used for normalization and relative quantification of gene expression and was performed according to the $\Delta\Delta$Ct method. Expression levels were represented in arbitrary units, calculated as a relative-fold increase compared with the control sample, arbitrarily set to 1. Quantitative RT-PCRs were repeated in triplicate from at least two independent experiments. The probes were supplied by Integrated DNA Technologies: *GAPDH*, Hs.PT39a.22214836, and *NR4A1,* Hs.PT.56a.20808305. In particular, the *NR4A1* probe sequence is 5′-/56-FAM/TCCAGAGTG/ZEN/AGATGCCCTGTATCCA/3IABkFQ/-3′; the *GAPDH* probe sequence is 5′-/56-FAM/AAGGTCGGA/ZEN/GTCAACGGATTTGGTC/3IABkFQ/-3′.

Fasudil Supplementation

Fasudil was purchased from Sigma-Aldrich (Cod. H139) and dissolved in deionized water; cells were treated for 24 hours with a final concentration of 10 μM. Morphometric studies were performed to quantitatively analyze the neuronal morphology. The iPSC-derived neurons were analyzed after immunofluorescence analysis for β-III-TUBULIN; morphometric measurements of length and number of neurites, number of branches per neurite, and average branching level were done by using MetaMorph image analysis software (Molecular Devices, Sunnyvale, CA, https://www.moleculardevices.com).

Endocytosis assays were performed by using the FM1-43 dye (Thermo Fisher Scientific Life Sciences) in cortical neuronal cultures. In particular, synapses from individual cortical neurons were labeled with FM1-43 [21]. Neurons were washed in a Tyrode buffer for 10 minutes and fixed in 4% paraformaldehyde in PBS for 10 minutes. After fixation, cells were incubated with VGluT-1 antibodies for detection of all synapses. Analyses were performed by quantification of the number of FM1-43 punctae colocalized with VGluT-1 and normalized to the neuron surface.

Statistical Analysis

All experiments were repeated at least three times as independent biological experiments. Data are expressed as mean and standard deviation. Comparisons between groups were performed by two-tailed unpaired Student *t* test; *p* values $<.05$ were considered to represent statistically significant differences. Data were analyzed by using Excel for Windows (Microsoft Corp, Redmond, WA, http://www.microsoft.com).

RESULTS

Abnormal Dendritic Morphology in Terminally Differentiated Cortical, Cerebellar, and Motor Neurons Derived From Human iPSCs Carrying *OPHN1* Loss-of-Function Mutations

To perform in vitro neurogenesis assays and analyze the cellular phenotype of OPHN1-deficient neurons, we generated iPSCs from two *OPHN1*-mutated patients (P1 and P2) and from two healthy controls fibroblast cell lines (C1 and C2) using the episomal reprogramming method (supplemental online Fig. 1A). iPSCs colonies from C1 and C2 showed a round appearance, whereas P1 and P2 had disorganized colony appearance with bipolar/tripolar and heterogeneous cellular morphology evident. P1 harbored a hemizygous G-to-C point mutation in the exon 4 splice site (IVS4+1G $>$ C mutation of *OPHN1*), whereas P2 harbored a two-base pair hemizygous deletion in the donor splice site

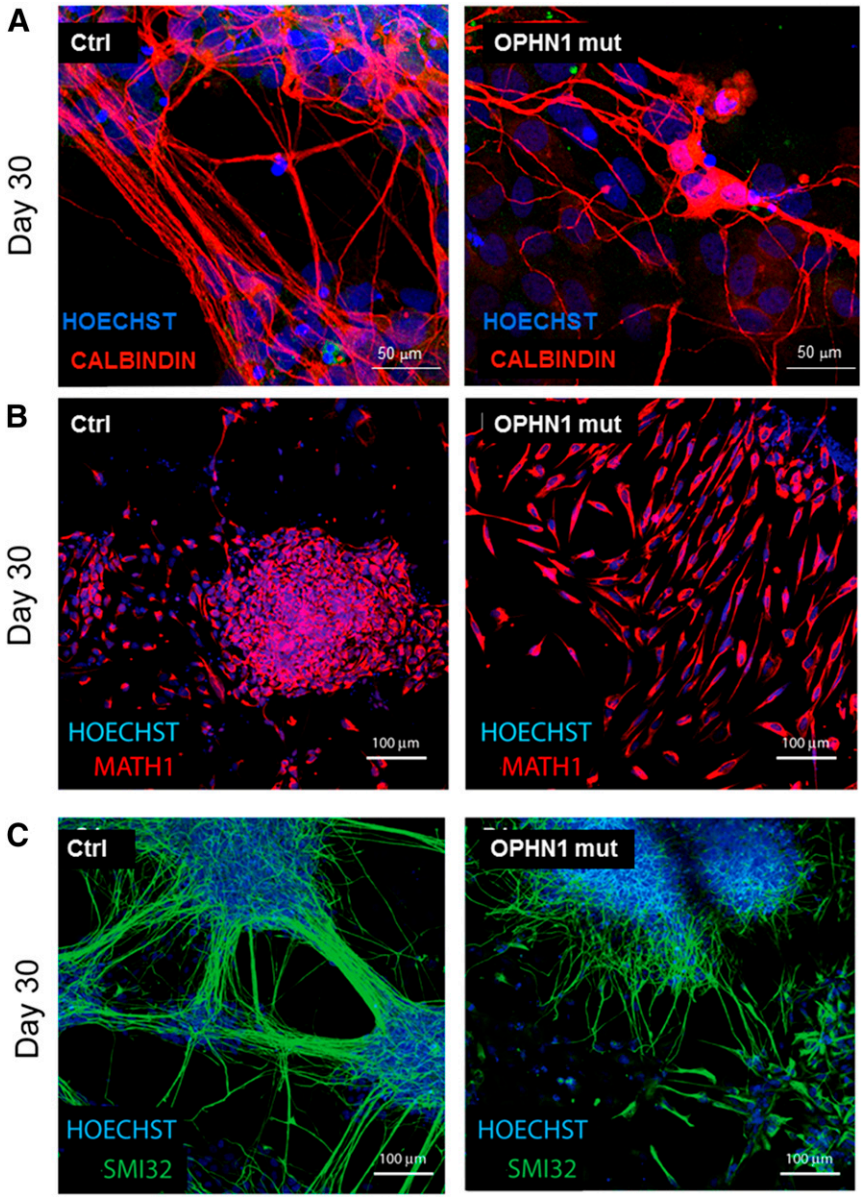

Figure 1. Morphological analysis of cortical, cerebellar, and motor neurons in Ctrl and *OPHN1*-mutated cells. Confocal images of immunofluorescence for CALBINDIN on cortical neurons **(A)**, MATH1 on cerebellar neurons **(B)**, and SMI32 on motor neurons after 30 days of differentiation **(C)**. The data obtained show that the *OPHN1*-mutated neurons (cortical, cerebellar, and motor neurons) present disrupted morphology in the absence of OPHN1 protein. Abbreviation: Ctrl, control; mut, mutant.

of exon 7 (IVS7+2,3del TA). The presence of *OPHN1* mutations was confirmed by direct sequencing (supplemental online Fig. 1B). The absence of OPHN1 protein was confirmed in P1 and P2 iPSCs through Western blot and immunofluorescence (supplemental online Fig. 1C, 1D). Three clones from each of the iPSC line were recovered and the colonies were positive for the markers of pluripotency: Oct4, Nanog, SSEA3, TRA-1-60, and alkaline phosphatase assay (supplemental online Fig. 2).

The neurogenic potential of the P1 and P2 iPSCs were assessed and compared with those of C1 and C2 iPSCs after specific protocols for differentiation into cortical, cerebellar granule, and motor neurons. The specific neuronal subtypes were confirmed through immunofluorescence analyses with markers of motor neurons (SMI32), markers of the cerebellar granule neurons (MATH1), and markers of the cortical neurons (CALBINDIN) (Fig. 1). The immunofluorescence data obtained with confocal microscopy showed that all neuronal subtypes obtained from P1 and P2 iPSCs had altered morphology. In particular, the cortical neurons obtained from control iPSCs displayed areas with multiple and elongated neurites that were not present in cultures of terminally differentiated cortical neurons obtained from *OPHN1*-mutated iPSCs (Fig. 1A). The cerebellar neurons derived from patients iPSCs displayed short neurites and a peculiar organization. In fact, neurites were oriented in a parallel manner that was not observed in control cerebellar neuronal cultures (Fig. 1B). The terminal differentiation of iPSCs into motor neurons showed that the neurites of *OPHN1*-mutated cells were shorter than control motor neurons (Fig. 1C). The terminal morphology observed in these three neuronal subtypes confirmed that *OPHN1*-mutated neurons showed an altered morphological phenotype.

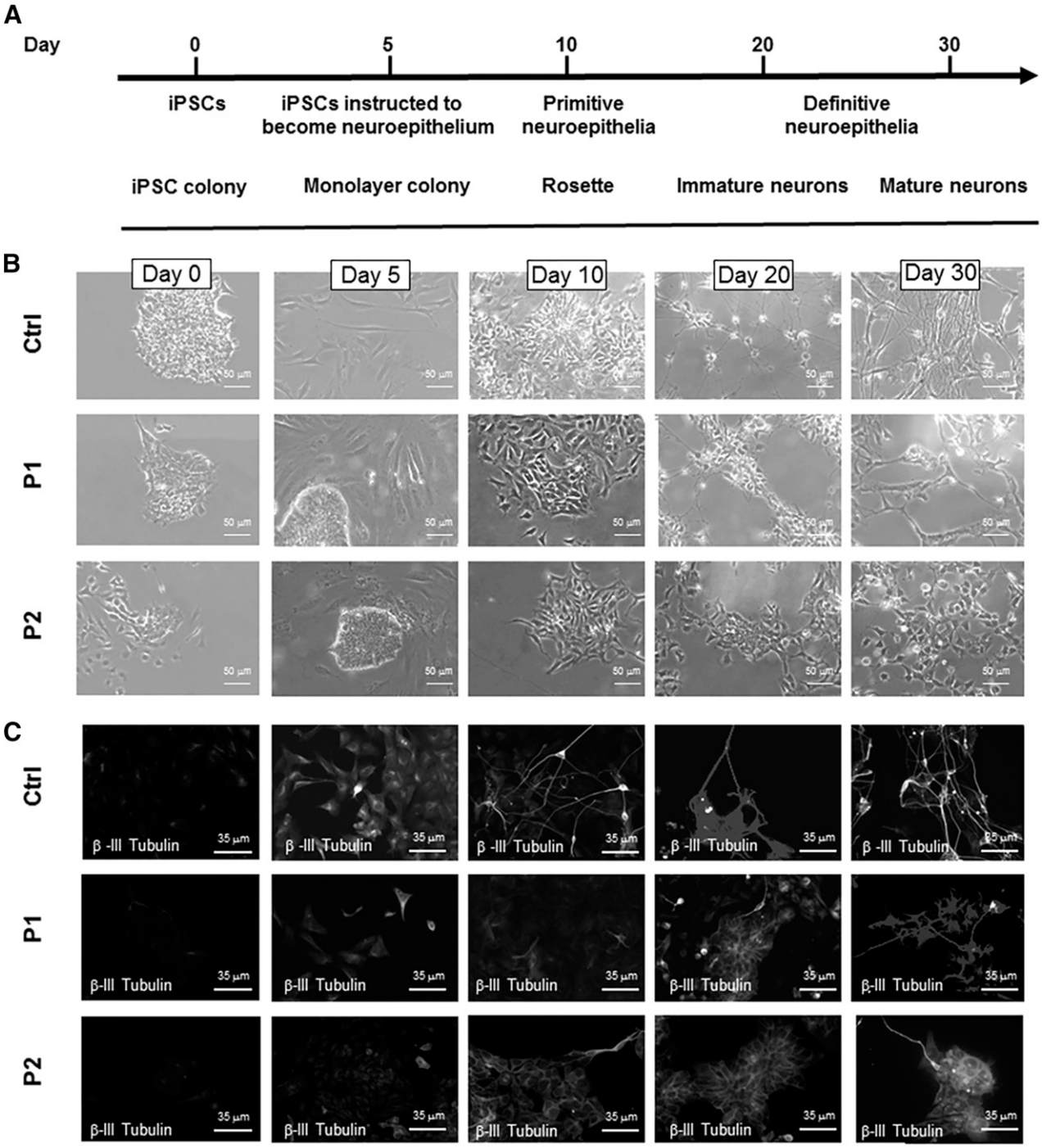

Figure 2. Analysis of control and patients' iPSC morphology during in vitro neurogenesis. Schemata of the neural differentiation procedure in vitro **(A)**. Representative images (of bright field photographs) showing morphological changes during neuronal differentiation of iPSCs derived from Ctrl, P1 and P2 subjects at different days of differentiation **(B, C)** and β-III TUBULIN immunofluorescence at the corresponding time (days 5, 10, 20, and 30 of in vitro neurogenesis). The data show that patients' cells present morphological alterations and delayed neuronal maturation. Abbreviations: Ctrl, control; IPSC, induced pluripotent stem cells; P, *OPHN1*-mutated iPSC lines.

Neuronal Maturation Defects in h-iPSC-Derived *OPHN1*-Mutated Cortical Neurons

The study of cortical neuronal differentiation of both P1 and P2 iPSCs showed that the number and the maturation of the developing neurons were altered compared with iPSCs derived from control individuals (Fig. 2). In particular, we calculated the percentage of differentiated neurons (by counting the number of β-III TUBULIN-positive cells over the total number of cells) and found that in P1 and P2 cultures at the end of day 30, the differentiation potential was reduced by 50%. In fact, in control cells the percentage of neurons was ~68.31 $\pm$ 8.67; this percentage was ~36.11 $\pm$ 9.29 in P1 and 26.94 $\pm$ 8.49 in P2 (supplemental online Fig. 3).

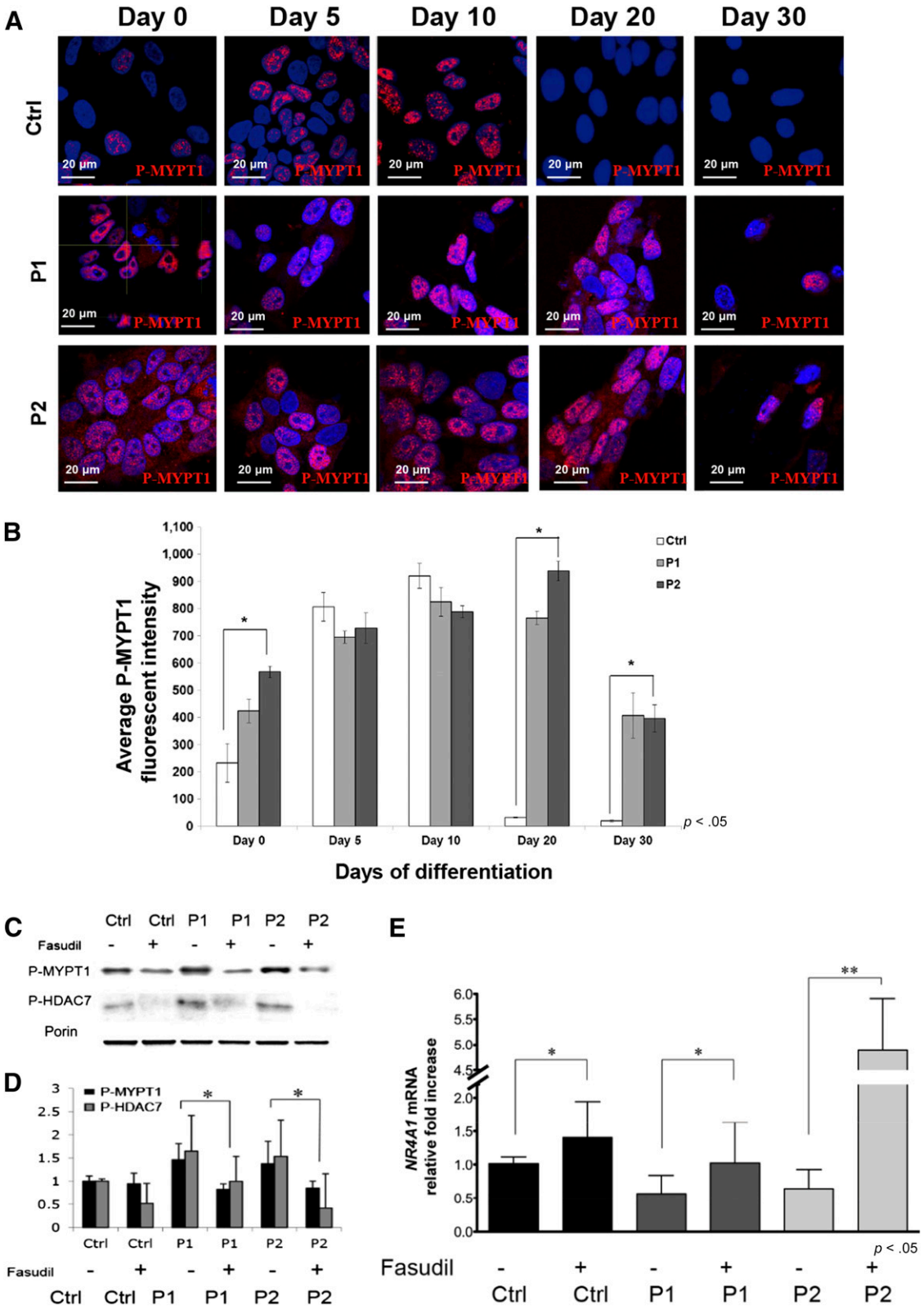

Figure 3. **(A):** Analysis of rho kinase (ROCK) activity in control and patients' induced pluripotent stem cells (iPSCs) during in vitro neurogenesis. P-MYPT1 immunofluorescence is shown at day 0, 5, 10, 20, and 30 of differentiation. Immunofluorescence analysis for P1 and P2 shows that P-MYPT1 is increased when compared with Ctrl and that it is retained throughout the differentiation process. **(B):** Quantification of P-MYPT1 fluorescent intensity in Ctrl, P1, and P2 cells before, during, and after neuronal differentiation. $*, p < .05$. **(C):** Western blot analysis of the activity of the ROCK signaling before and after treatment with the ROCK inhibitor (fasudil 10 μM) in Ctrl and *OPHN1*-mutated iPSCs. The effect of fasudil (*Figure legend continues on next page*.)

Since day 5 of neuronal differentiation, it was evident that in patients' cultures, the cellular morphology still resembled those of proliferating iPSCs where colonies were still present. At day 10, control cultures formed the characteristic structure of the neuronal rosette. In the patients' cultures, the neuronal rosettes showed altered morphology. Moreover, at day 20, well-developed neurons were present in control cultures, whereas in the patients' cultures showed decreased and delayed development of β-III TUBULIN-positive neurons (at day 30). These results suggested that during in vitro neurogenesis the *OPHN1*-mutated iPSCs had morphological alterations and delayed maturation.

Modulation of ROCK Signaling During In Vitro Neurogenesis Was Disrupted in Neurons With *OPHN1* Loss of Function

To study ROCK signaling during in vitro neurogenesis of cortical neurons, we investigated the phosphorylation status of the substrate protein MYPT1 on Thr-853 because it gives a readout of ROCK activity [22]. Importantly, high levels of P-MYPT1 indicate high ROCK activity, which is considerably increased in *OPHN1*-mutated cells compared with control cell levels (Fig. 3A). Immunofluorescence studies (Fig. 3A) and fluorometric quantification (performed on 170 cells per specimen) (Fig. 3B) showed that during in vitro neurogenesis of control iPSCs, the levels of P-MYPT1 increased until day 10 and then decreased through the final steps of differentiation (days 20 and 30) (the average intensity of fluorescent signal changed from 233.22 $\pm$ 71.11 at day 0 to 806.72 $\pm$ 52.47, 920.83 $\pm$ 46.51, 31.83 $\pm$ 2.0, and 19.16 $\pm$ 3.66 at days 5, 10, 20, and 30, respectively). In contrast, in patients' iPSCs the levels of P-MYPT1 remained high throughout differentiation (the average intensity signal of P-MYPT1 fluorescence was 424.52 $\pm$ 43.37 at day 0, 694.87 $\pm$ 22.46 at day 5, 825.23 $\pm$ 53.48 at day 10, 766.24 $\pm$ 24.78 at day 20, 407.21 $\pm$ 82.90 at day 30 for P1 and 567.43 $\pm$ 2,115 at day 0, 728.92 $\pm$ 55.56 at day 5, 788.40 $\pm$ 22.37 at day 10, 938.61 $\pm$ 35.83 at day 20, and 395.93 $\pm$ 49.98 at day 30 for P2). Our results indicated that biochemical disruption of ROCK signaling observed in P1 and P2 neurogenesis likely contributed to immaturity of the neuronal morphology.

To further confirm the importance of ROCK signaling on neuronal differentiation and morphology, we exposed control (wild-type) proliferating iPSCs to 10 μm fasudil for 24 hours and observed significant changes in cell morphology; not only did iPSCs acquire a neuronal-like morphology but they also became positive for β-III-TUBULIN (supplemental online Fig. 4A, 4B). We counted the number of β-III-TUBULIN cells over the total number of cells in culture and observed that whereas in untreated conditions the number of cells spontaneously differentiating into neurons is below 3% (2.86 $\pm$ 1.79; after 1 day of fasudil supplementation, the percentage increased to 15% (16.56 $\pm$ 3.27) (350 cells examined; n = 3 experiments) (supplemental online Fig. 4C).

Treatment With Fasudil Rescued ROCK Levels and Downstream Expression of Neurotrophic *NR4A1* of h-iPSCs Derived From OPHN1-Defective Neurons

To validate the efficacy of the treatment with the ROCK inhibitor fasudil, we supplemented P1 and P2 cells with 10 μM of fasudil to rescue the OPHN1-defective phenotype. By Western blot assay, we showed that P-MYPT1 levels decreased in both P1 and P2 iPSCs after ROCK inhibition (Fig. 3C). These results suggested that treatment of OPHN1-deficient cells with fasudil re-established the activity of the ROCK pathway to levels similar to those in control iPSCs, as also shown by densitometric analysis performed on Western blot (Fig. 3D). In addition to the effect that fasudil had on P-MYPT1, our results also indicated that the phosphorylation levels of histone deacetylase 7 (HDAC7) are dependent on ROCK. In fact, P-HDAC7 levels decreased after fasudil treatment in control, P1, and P2 iPSCs.

ROCK signaling, which is hyperactivated in OPHN1-defective iPSCs, controls nucleocytoplasmic shuttling of HDAC7 and modulates the expression of its target gene *NR4A1* [25]. We assessed whether treatment with fasudil could restore the expression of *NR4A1* to control levels. Quantitative PCR analyses of *NR4A1* mRNA levels in control, P1, and P2 iPSCs, showed that decreased *NR4A1* levels in P1 and P2 were rescued after fasudil treatment in both P1 and P2 (Fig. 3E).

Treatment With Fasudil Restored Neuronal Morphology in h-iPSC-Derived OPHN1-Deficient Neurons

To perform quantitative analyses, we tested the effects of fasudil on low-density neuronal cortical neurons, in which the neurites and branching level of each neuron are clearly visible (at day 30 of differentiation). The results obtained from three independent experiments showed that fasudil treatment of P1 and P2 differentiated cortical neurons rescued the altered neuronal morphology of OPHN1-deficient neurons (Fig. 4A). In fact, after treatment the average neurite length increased from $\sim$65.51 μm to $\sim$131.97 μm in P1 and from $\sim$58.44 μm to $\sim$128.77 μm in P2, whereas in control cortical neurons the average neurite length changed from $\sim$148.60 μm to $\sim$155.97 μm (150 cells examined; n = 3 experiments; $p < .05$). The number of branches, which indicates the maturation level of the neurons, increased from $\sim$1.41 to $\sim$3.2 in P1 and from $\sim$1.31 to $\sim$2.4 in P2, whereas in control cortical neurons the number of branches increased from $\sim$2.23 to $\sim$2.91 (150 cells examined; n = 3 experiments; $p < .05$). The branching level, which also indicates the maturation level of the neuronal culture, was decreased in P1 and P2 cultures compared with control cultures; importantly, it was also rescued to control levels by treatment with fasudil ($\sim$0.04 to $\sim$0.81 in P1 and $\sim$0.02 to 0.77 in P2 and from $\sim$0.34 to 0.62 in control cells) (150 cells examined; n = 3 experiments; $p < .05$) (Fig. 4B).

(*Figure legend continued from previous page*.)
is shown on P-MYPT1 and P-HDAC7 in Ctrl, P1, and P2 iPSCs. **(D):** Densitometric analysis of protein extract obtained from (proliferating) iPSCs from Ctrl and patients (P1, P2) after 1 day of treatment. *, $p < .05$. **(E):** Quantitative polymerase chain reaction analysis of *NR4A1* transcripts levels showing that they are decreased in P1 and P2 but rescued after fasudil treatment. Data (mean + SD of three independent experiments) are expressed as fold increase of versus Ctrl cells, using glyceraldehyde 3-phosphate dehydrogenase as standard control. These data show that ROCK hyperactivity parallels reduced *NR4A1* levels and that the ROCK inhibitor fasudil is able to increase the reduced *NR4A1* levels to control levels in P1 and above control level in P2. *, $p < .05$; **, $p < .005$. Statistical analysis was performed when each group had at least three samples with the unpaired t test. $p < .05$ was considered to indicate a significant difference; *, $p < .05$; **, $p < .005$. All results are presented as mean $\pm$ SD. Abbreviations: Ctrl, control; HDAC7, histone deacetylase 7; P-MYPT1, myosin phosphatase targeting subunit 1; P, *OPHN1*-mutated iPSC lines.

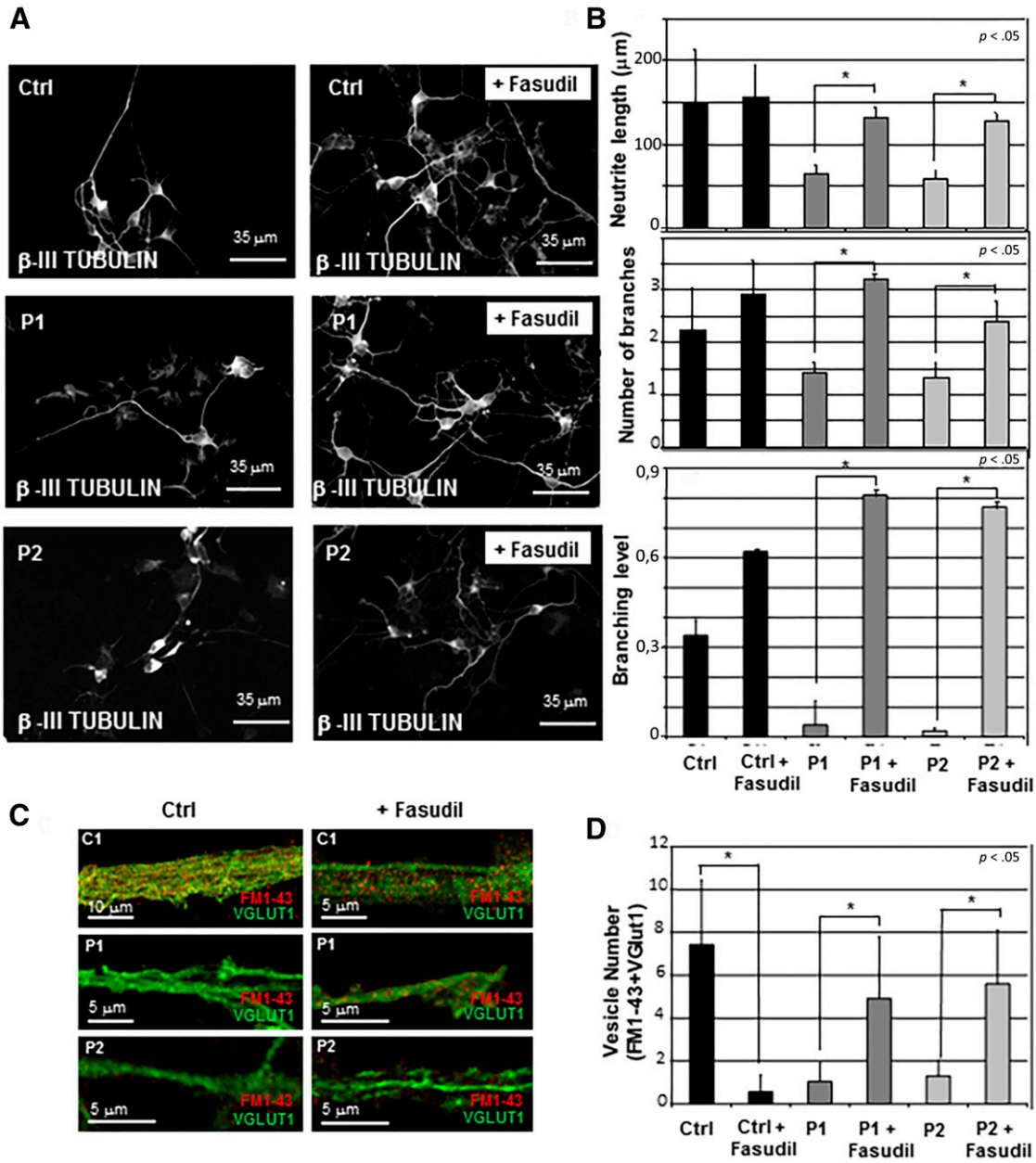

Figure 4. Morphological analysis and functional endocytosis assays in Ctrl, P1, and P2 neuronal cultures before and after fasudil treatment. **(A):** Immunofluorescence images of β-III TUBULIN neuronal cultures at the end of differentiation (day 30) showing that the patients' cultures have a decreased neurite length and fewer branches. Importantly, after fasudil treatment, the length and the number of branches increased. **(B):** Quantitative analysis of the immunofluorescence images. $*$, $p < .05$. **(C):** Analysis of FM1-43 uptake in neurites of cortical neurons before and after ROCK inhibition with fasudil. Neurons were stimulated by high potassium buffer in the presence of FM1-43 dye. FM1-43 punctae (in red) that colocalized with the presynaptic protein VGLUT1 (in green) on individual neurites indicate the efficiency of endocytosis. Interestingly, the patients' neurites have decreased positivity to FM1-43, but fasudil treatment re-established the FM1-43 punctae in P1 and P2 neurites to levels similar to that in the Ctrl. **(D):** Quantitative analysis of the FM1-43 uptake reporting only the FM1-43 puncta that colocalized with VGLUT1. Statistical analysis was performed when each group had at least three samples with the unpaired *t* test. $p < .05$ was considered to indicate a significant difference; $*$, $p < .05$; $**$, $p < .005$. All results are presented as mean $\pm$ SD. Abbreviations: Ctrl, control; P, *OPHN1*-mutated iPSC lines.

Treatment With Fasudil Increased SVE Close to Control Levels

Data from ophn1 mutant mice showed that SVE was reduced in hippocampal neurons [8]. We studied the uptake of FM1-43, a fluorescent amphipathic-styryl dye in individual synapses from cortical neurons derived from *OPHN1*-mutated patients (P1 and P2) after potassium stimulation and detected an average reduction of 75% in FM1-43/VGlut1-positive puncta compared with control neurons ($n = 3$ experiments; $p < .05$) (Fig. 4C). To quantify these data, we counted the number of FMI-43 vesicle positive for VGLUT1, indicating the endocytotic synaptic vesicle, and found that this number increased from ~1.04 to ~4.91 in P1 and from

~1.3 to ~5.6 in P2 and decreased from ~7.43 to ~0.56 in control cells (Fig. 4D).

Discussion

In vitro and in vivo studies on hippocampal neurons of *ophn1*-deficient mice have shown an increase in immature dendritic protrusions (filopodia) and reduced mature spine density in cultured differentiated hippocampal and cortical neurons. Phenotypic characterization of the OPHN1 knockout mouse has revealed behavioral defects in spatial memory, impairment in social interaction, and hyperactivity. At the anatomic level, cerebral ventricle dilatation is present as in the human phenotype, whereas cerebellar defects have not been observed [11]. An overview of behavioral and learning deficits in *OPHN1*-mutated patients analyzed in the present study is provided in supplemental online Table 1. Terminally differentiated cortical neurons derived from patients with *OPHN1* loss of function showed an immature neuronal phenotype and a reduction in synaptic vesicle internalization. The abnormalities observed during in vitro neurogenesis of h-iPSCs occurred at early stages of neuronal development and are likely due to persistently elevated ROCK activity, with consequences at multiple levels due to the phosphorylation of several key factors. These factors include not only MYPT1 and MLCK but also vimentin LIMK (lin-11, Isl-1 mec-3 kinase), vimentin, and other proteins influencing cytoskeletal rearrangements at all stages of neuronal development [23]. ROCK additionally phosphorylates endophilin A1, a protein implicated in membrane curvature generation in clathrin-mediated SVE, inhibiting it by disruption of its interaction with CIN85 [24]. Interestingly, OPHN1 interacts with both endophilin A1 and Cbl-interacting protein of 85 kDa [11]. We have recently demonstrated that high levels of P-MYPT1 trigger phosphorylation of class II HDAC7, with consequences on the nuclear import of this transcriptional repressor and downregulation of the neurotrophic factor *NR4A1* in OPHN1 patients' iPSCs [25]. This could also contribute to the abnormalities in neurite outgrowth and dendritic immaturity. Therefore, in addition to the effect that fasudil has on P-MYPT1, our results indicate that phosphorylation levels of HDAC7 are dependent on ROCK activity. In fact, after fasudil treatment, P-HDAC7 levels decreased and NR4A1 expression was rescued to control levels.

Fasudil hydrochloride (HA1077) is a isoquinoline sulfonamide derivative that inhibits ROCK by binding to a hydrophobic cleft in its catalytic domain [26]. Fasudil is used in clinic for preventing cerebral vasospasm after subarachnoid hemorrhage and symptoms of cerebral ischemia. Recent studies showed that fasudil also promotes the survival of neural stem cells, axonal regeneration and neuronal differentiation of bone marrow mesenchymal cells [27].

Fasudil is not only a ROCK inhibitor but also a potent protein kinase A (PKA) inhibitor [28]. The interplay between PKA and ROCK was already known and has recently been documented, confirming ROCK as a substrate of PKA in vivo and in vitro [29, 30]. Moreover, dysregulation of PKA signaling was demonstrated in mice with constitutive lack of *ophn1* [31]. It is therefore not surprising that a reduction of ROCK level by fasudil might have consequences on endocytosis that are independent of MYPT1 phosphorylation levels, possibly through PKA and ROCK interactions that need to be explored in the future. Interestingly, the administration of fasudil to control cells drastically reduces synaptic vesicle number, despite the reduction of P-MYPT1 levels, whereas in patient cells endocytosis is enhanced by ROCK inhibition.

A series of studies have demonstrated that ROCK inhibition is efficacious in animal models of stroke, multiple sclerosis, amyotrophic lateral sclerosis, Alzheimer's disease, and Parkinson's disease (reviewed by Hensel et al. 32]). The ROCK pathway is a key therapeutic target in neurodegenerative and neurotraumatic disorders, and ROCK inhibitors should be promising drugs for preventing neurodegeneration and stimulating neuroregeneration. The restoration of the neuronal phenotype in the h-iPSC-derived model of OPHN1 syndrome makes fasudil a valid therapeutic option for human neurodevelopmental disorders due to OPHN1 dysfunction and potentially for other conditions with hyperactivation of the RhoA/ROCK pathway.

The ROCK pathway is essential to neurogenesis, as demonstrated by LPA, which hyperactivates the pathway and inhibits neuronal differentiation and expansion of hESCs, whereas ROCK inhibition promotes neurite outgrowth in adipose stem cells. We tested the effects of fasudil supplementation on fibroblast-derived human iPSCs, confirming that ROCK inhibition favors neuronal differentiation.

The analysis of the levels of ROCK activity at different stages of human iPSCs in vitro neurogenesis revealed that there is a precise modulation (which is lost in OPHN1-deficient cells) and that starting at day 10 ROCK activity progressively decreases in parallel with morphological changes and upregulation of neurotrophic factor *NR4A1.*

Conclusion

We showed the morphological, biochemical, and functional features of human OPHN1-deficient iPSCs characterized by hyperactive ROCK signaling and their rescue by treatment with the ROCK inhibitor fasudil. These findings shed light on the relevance of the ROCK pathway during in vitro neuronal differentiation in physiology and disease, not only through morphological changes due to cytoskeletal reorganization but also through epigenetic regulation that allows transcription of genes that are relevant for neuronal differentiation and survival, such as *NR4A1*. Thus, it provides a neuronal model for human OPHN1 syndrome and its treatment.

Acknowledgments

We thank Dr. Stefania Corti for helpful technical advice on iPSCs differentiation protocols and Rossella Borghi for experimental support. We also thank the patients and the families for their enthusiastic support of our research. This work was funded by the Pierfranco e Luisa Mariani Foundation (project R-12-91) and Italian Telethon (project GGP01845).

Author Contributions

C.C.: conception and design, collection and/or assembly of data, data analysis and interpretation, manuscript writing; S.B., S.P., G.P., and P.A.: provision of study material or patients, collection and/or assembly of data; P.B. and P.C.: data analysis and interpretation; E.B.: provision of study material or patients, data analysis and interpretation; G.Z.: conception and design, provision of study material or patients, data analysis and interpretation, manuscript writing, final approval of manuscript.

Disclosure of Potential Conflicts of Interest

The authors indicated no potential conflicts of interest.

REFERENCES

1 Eccles JC. Neurogenesis and morphogenesis in the cerebellar cortex. Proc Natl Acad Sci USA 1970;66:294–301.

2 Luo L. Rho GTPases in neuronal morphogenesis. Nat Rev Neurosci 2000;1:173–180.

3 Seko T, Ito M, Kureishi Y et al. Activation of RhoA and inhibition of myosin phosphatase as important components in hypertension in vascular smooth muscle. Circ Res 2003;92:411–418.

4 Linseman DA, Hofmann F, Fisher SK. A role for the small molecular weight GTPases, Rho and Cdc42, in muscarinic receptor signaling to focal adhesion kinase. J Neurochem 2000;74: 2010–2020.

5 Billuart P, Bienvenu T, Ronce N et al. Oligophrenin-1 encodes a rhoGAP protein involved in X-linked mental retardation. Nature 1998;392:923–926.

6 Philip N, Chabrol B, Lossi AM et al. Mutations in the oligophrenin-1 gene (OPHN1) cause X linked congenital cerebellar hypoplasia. J Med Genet 2003;40:441–446.

7 Zanni G, Saillour Y, Nagara M et al. Oligophrenin 1 mutations frequently cause X-linked mental retardation with cerebellar hypoplasia. Neurology 2005;65:1364–1369.

8 Khelfaoui M, Pavlowsky A, Powell AD et al. Inhibition of RhoA pathway rescues the endocytosis defects in Oligophrenin1 mouse model of mental retardation. Hum Mol Genet 2009;18: 2575–2583.

9 Nadif Kasri N, Nakano-Kobayashi A, Malinow R et al. The Rho-linked mental retardation protein oligophrenin-1 controls synapse maturation and plasticity by stabilizing AMPA receptors. Genes Dev 2009;23:1289–1302.

10 Powell AD, Gill KK, Saintot PP et al. Rapid reversal of impaired inhibitory and excitatory transmission but not spine dysgenesis in a mouse model of mental retardation. J Physiol 2012;590:763–776.

11 Khelfaoui M, Denis C, van Galen E et al. Loss of X-linked mental retardation gene oligophrenin1 in mice impairs spatial memory and leads to ventricular enlargement and dendritic spine immaturity. J Neurosci 2007;27: 9439–9450.

12 Watanabe K, Ueno M, Kamiya D et al. A ROCK inhibitor permits survival of dissociated human embryonic stem cells. Nat Biotechnol 2007;25:681–686.

13 Xue ZW, Shang XM, Xu H et al. Rho-associated coiled kinase inhibitor Y-27632 promotes neuronal-like differentiation of adult human adipose tissue-derived stem cells. Chin Med J (Engl) 2012;125:3332–3335.

14 Frisca F, Crombie DE, Dottori M et al. Rho/ROCK pathway is essential to the expansion, differentiation, and morphological rearrangements of human neural stem/progenitor cells induced by lysophosphatidic acid. J Lipid Res 2013;54:1192–1206.

15 Pirozzi F, Di Raimo FR, Zanni G et al. Insertion of 16 amino acids in the BAR domain of the oligophrenin 1 protein causes mental retardation and cerebellar hypoplasia in an Italian family. Hum Mutat 2011;32:E2294–E2307.

16 Yamashita K, Kotani Y, Nakajima Y et al. Fasudil, a Rho kinase (ROCK) inhibitor, protects against ischemic neuronal damage in vitro and in vivo by acting directly on neurons. Brain Res 2007;1154:215–224.

17 Compagnucci C, Nizzardo M, Corti S et al. In vitro neurogenesis: Development and functional implications of iPSC technology. Cell Mol Life Sci 2014;71:1623–1639.

18 Zeng H, Guo M, Martins-Taylor K et al. Specification of region-specific neurons including forebrain glutamatergic neurons from human induced pluripotent stem cells. PLoS One 2010;5:e11853.

19 Erceg S, Lukovic D, Moreno-Manzano V et al. Derivation of cerebellar neurons from human pluripotent stem cells. Curr Protoc Stem Cell Biol 2012;Chapter 1:Unit 1H.5.

20 Corti S, Nizzardo M, Simone C et al. Genetic correction of human induced pluripotent stem cells from patients with spinal muscular atrophy. Sci Transl Med 2012;4:165ra162.

21 Mozhayeva MG, Sara Y, Liu X et al. Development of vesicle pools during maturation of hippocampal synapses. J Neurosci 2002;22: 654–665.

22 Ito M, Nakano T, Erdodi F et al. Myosin phosphatase: Structure, regulation and function. Mol Cell Biochem 2004;259:197–209.

23 Julian L, Olson MF. Rho-associated coiled-coil containing kinases (ROCK): Structure, regulation, and functions. Small GTPases 2014;5: e29846.

24 Kaneko T, Maeda A, Takefuji M et al. Rho mediates endocytosis of epidermal growth factor receptor through phosphorylation of endophilin A1 by Rho-kinase. Genes Cells 2005;10: 973–987.

25 Compagnucci C, Barresi S, Petrini S et al. Rho-kinase signaling controls nucleocytoplasmic shuttling of class IIa histone deacetylase (HDAC7) and transcriptional activation of orphan nuclear receptor *NR4A1*. Biochem Biophys Res Commun 2015;459:179–183.

26 Yamaguchi H, Kasa M, Amano M et al. Molecular mechanism for the regulation of rho-kinase by dimerization and its inhibition by fasudil. Structure 2006;14:589–600.

27 Ding J, Yu JZ, Li QY et al. Rho kinase inhibitor Fasudil induces neuroprotection and neurogenesis partially through astrocyte-derived G-CSF. Brain Behav Immun 2009;23: 1083–1088.

28 Breitenlechner C, Gassel M, Hidaka H et al. Protein kinase A in complex with Rho-kinase inhibitors Y-27632, Fasudil, and H-1152P: structural basis of selectivity. Structure 2003;11: 1595–1607.

29 Leemhuis J, Boutillier S, Schmidt G et al. The protein kinase A inhibitor H89 acts on cell morphology by inhibiting Rho kinase. J Pharmacol Exp Ther 2002;300:1000–1007.

30 Hamaguchi T, Nakamuta S, Funahashi Y et al. In vivo screening for substrates of protein kinase A using a combination of proteomic approaches and pharmacological modulation of kinase activity. Cell Struct Funct 2015;40:1–12.

31 Khelfaoui M, Gambino F, Houbaert X et al. Lack of the presynaptic RhoGAP protein oligophrenin1 leads to cognitive disabilities through dysregulation of the cAMP/PKA signalling pathway. Philos Trans R Soc Lond B Biol Sci 2013;369:20130160.

32 Hensel N, Rademacher S, Claus P. Chatting with the neighbors: crosstalk between Rho-kinase (ROCK) and other signaling pathways for treatment of neurological disorders. Front Neurosci 2015;9:198.

See www.StemCellsTM.com for supporting information available online.